Water vapor pressure over molten KH2PO4 and demonstration of water electrolysis at 300ºC

Berg, Rolf W.; Nikiforov, Aleksey Valerievich; Petrushina, Irina; Bjerrum, Niels J.

Published in:
Applied Energy

Link to article, DOI:
10.1016/j.apenergy.2016.07.123

Publication date:
2016

Document Version
Peer reviewed version

Water vapor pressure over molten KH_2PO_4 and demonstration of water electrolysis at ~300 °C

R. W. Berg[a*], A. V. Nikiforov[b], I.M. Petrushina[b] and N. J. Bjerrum[b]

[(a)] DTU Chemistry, Technical University of Denmark, Kemitorvet, 207, DK–2800 Kgs. Lyngby, Denmark, rwb@kemi.dtu.dk
[(b)] DTU Energy, Same University and address, nava@dtu.dk, irpe@dtu.dk, nibj@dtu.dk

Highlights

- The vapor pressure over molten KH_2PO_4 was measured by Raman spectroscopy to be about 8 bars at ~300 °C.
- Raman spectroscopy shows that molten KH_2PO_4 under its own vapor pressure contains much dissolved water.
- It is demonstrated spectroscopically that water electrolysis is possible in KH_2PO_4 electrolyte forming H_2 and O_2 at 300 °C.
- Molten KH_2PO_4 is a possible electrolyte for water electrolysis.

Abstract

A new potentially high-efficiency electrolyte for water electrolysis: molten monobasic potassium phosphate, KH_2PO_4 or KDP has been investigated at temperatures ~275–325 °C. At these temperatures, KH_2PO_4 was found to dissociate into H_2O gas in equilibrium with a melt mixture of KH_2PO_4–$K_2H_2P_2O_7$–KPO_3–H_2O. The water vapor pressure above the melt, when contained in a closed ampoule, was determined quantitatively *vs.* temperature by use of Raman spectroscopy with methane or hydrogen gas as an internal calibration standard, using newly established relative ratios of Raman scattering cross sections of water and methane or hydrogen to be 0.40 ± 0.02 or 1.2 ± 0.03. At equilibrium the vapor pressure was much lower than the vapor pressure above liquid water at the same temperature. Electrolysis was realized by passing current through closed ampoules (vacuum sealed quartz glass electrolysis cells with platinum electrodes and the electrolyte melt). The formation of mixtures of hydrogen and oxygen gases as well as the water vapor was detected by Raman spectroscopy. In this way it was demonstrated that water is present in the new electrolyte: molten KH_2PO_4 can be split by electrolysis via the reaction $2\ H_2O \rightarrow 2\ H_2 + O_2$ at temperatures ~275–325 °C. At these temperatures, before the start of the electrolysis, the KH_2PO_4 melt gives off H_2O gas that pressurizes the cell according to the following dissociations: $2\ KH_2PO_4 \leftrightarrow K_2H_2P_2O_7 + H_2O \leftrightarrow 2\ KPO_3 + 2\ H_2O$. The spectra show however that the water by virtue of hydrogen-bonding has a high affinity for remaining in the melt. The formed hydrogen and oxygen gasses were detected by means of the characteristic Raman gas-phase spectra.

Keywords: Molten salt electrolyte; KDP; Elevated temperature water electrolysis; Vapor pressure; Phosphate-based electrolytes; Raman spectroscopy; Water electrolysis.

1. Introduction

Efficient supply of enough energy - in a sustainable way - is essential for the modern society. Fossil fuels cannot be continuously used and renewable sources must be devised. Electrolysis of water to form hydrogen and oxygen is considered to be an important way to construct future renewable energy storage and conversion (load-leveling) systems. Electrical energy efficiency is essential in the formation of the 2 H_2 + O_2 gas mixture via water electrolysis. We tried in the present work to see if electrolysis could be performed at elevated temperatures utilizing a novel intermediate temperature electrolyte. The ΔG of the water splitting reaction is falling by ~6 % from room temperature to 325 ^oC giving possibilities for somewhat more efficient electrolyses, but the main benefit in our opinion of the use of higher temperatures is a better opportunity of applying non-precious catalysts for the electrode processes.

At temperatures higher than ~100 °C however the liquid water tends to evaporate easily, if not pressurized. Electrolysis in the gas phase is not particularly suitable and applications of high temperature liquids that contain water are preferred; among those are certain molten salts such as KH_2PO_4. The KH_2PO_4 (or KDP) salt has various applications [1] and recently also the use of the melt as an electrolyte for high temperature water electrolysis was suggested [2]. Upon the melting process water molecules are considered to participate in formation of eutectic mixtures with phosphates and other salts, due to reactions like e. g. 2 KH_2PO_4 $\leftrightarrow$ $K_2H_2P_2O_7 + H_2O$ $\leftrightarrow$ 2/n $(KPO_3)_n$ + 2 H_2O for (n = 1, 2, 3, ….) [3,4] whereby the melt loses water by evaporation, starting at ~180 °C [5]. Further heating of the system under open atmosphere will inevitably decompose it to the metaphosphate salt $(KPO_3)_n$ and water vapor. The KH_2PO_4 melt binds water via hydrogen bonds [6] and is known to be a proton conducting electrolyte [1,7]. In the present work we therefore tried applying it for water electrolysis since preliminary studies in this connection have shown promising results for the conductivity of several molten KH_2PO_4 salt mixtures with more or less water at temperatures of 240-320 °C under their own water vapor pressures [1]. In that article conductivity data for KH_2PO_4-H_2O and KH_2PO_4-KPO_3 systems were given as polynomial functions of temperature and composition, and it was shown that the KH_2PO_4 melts have high conductivities, in the order of ~0.30 S cm^{-1} at ~300 °C, and thus constitute promising electrolytes for pressurized water electrolysis at elevated temperatures. The melting point of the KH_2PO_4 electrolyte under its vapor pressure in a small volume was determined to be ~272 °C [1], although lower melting point values around ~253 °C often have been reported in the literature [8,9]. There is evidently no true melting point when open to the ambient atmosphere, as fusion is simultaneously accompanied by decomposition due to loss of water, as shown by an evolution of gas (water vapor) from the crystals [10].

The detailed in-situ stability of the electrolyte at high temperatures (~150–400 °C) was in focus, here manifested via the vapor pressure curve of water over the melt up to ~325 °C. There seems to be essentially no vapor pressure data known for the system. Finally, the purpose of the present work was to demonstrate *in-situ* formation of hydrogen and oxygen at temperatures as high as ~325 °C. This demonstration was an essential part of the work. Such information has never been obtained before and is an important prerequisite before study and optimization of the high temperature water electrolysis application can be done. Such work is now under planning in our research group.

The applied Raman spectroscopy experiments reported here consisted of sending laser beams directly through the samples in ampoules and deducting the chemical situation from the spectra and other observations. In this way we obtained remarkable new results on the vapor pressure and the electrolytic splitting of the water.

2. Experimental, Materials and Methods

Chemicals. Well crystallized monobasic potassium phosphate, KH_2PO_4 was used as received (CAS #7778-77-0 from Sigma, Japan, Pcode 101092922, PO662-500G, Lot# 031M0033V, purity > 99.9 %, melting at about 272 ±1 °C according to our results when freshly sealed in ampoule with little free volume [1]). Methane and hydrogen (>99.9% pure gasses) were obtained from AGA/Linde, Copenhagen S, DK and S. Frederiksen, Ølgod, DK. The Raman spectra showed no trace impurities, confirming that the salt and the gases were clean and dry.

Raman spectral method. Horizontal laser beams were sent into or through solid, molten or gaseous samples in vertically placed home-made ampoules (cells) to let the chemical situation be remotely and directly deduced from Raman scattered light or from other observations. A DILOR–XY 800 mm focal-length Raman spectrometer with a macroscopic sampling stage from Horiba–Jobin–Yvon, Ltd. was used. Excitation was done with a 532 nm green laser (a Spectra–Physics Millennia IIs module based on a 1064 nm Nd:YVO_4 laser with a crystalline LiB_3O_5 frequency–doubling device) with a power setting at < 3.5 W (vertically polarized). The light was collected through a 5 $cm^{Ø}$ wide achromatic lens of 10 cm focal length. The 90° scattered Rayleigh light was filtered off through a SuperNotch–Plus filter (Kaiser Optical Systems, Inc.). A quarter wave plate mounted before the entrance slit depolarized the light to make the grating efficiency independent of the polarization properties of the remaining light. The slits were opened to widths of 0.5 mm and lengths of 10 mm to obtain better signals at the expense of the resolution (about 8 cm^{-1}). The spectrometer was of Czerny–Turner type with spherical mirrors and with a 10 × 10 cm^2 1800 groves/mm plane holographic grating [11] dispersed and focused the light on to a Jobin-Yvon Synapse™ CCD detector (1024 × 256 pixels) with thermoelectric cooling (-70 °C) running under Horiba Scientific Labspec™ 5.42 software. The Raman signals were not calibrated for the quantum efficiency of the CCD response versus wavelength, but the spectrometer cm^{-1} scale was checked by use of neon emission lines and liquid cyclohexane Raman bands [12]. Intensity data for the spectral lines were measured several times for many minutes with an intensive excitation beam (acquisition time up to 5 x 600 s with automatic removal of cosmic spikes). In order to obtain reliability the measurements were repeated, averaged, scaled and shifted with the Labspec software but not further corrected. Other experimental details have been described elsewhere [13, 14].

Furnace. Some measurements were done at room temperature, others at higher temperatures in a range from ~50 °C to ~350 °C. The heating was done by use of a home-made aluminium-bronze core electrical furnace with four silica windows, see Fig. 1. The windows were covered with steel nets to protect the Raman instrument and the surroundings against ampoule explosion. Be aware that high temperatures may give considerable risk of explosions because of high internal pressures which develop inside ampoules. Temperatures were determined with several thermocouples and two 4-wire-Pt-100-Ω resistors to a precision better than ~1 °C, but the temperature inside the furnace was only precise to ~2 °C due to temperature gradients.

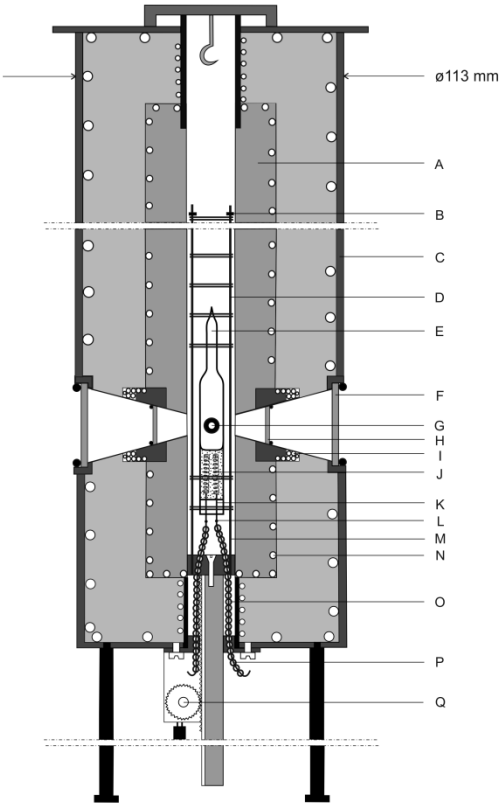

Fig. 1. Raman furnace with four windows used for vapor pressure or electrolysis measurements: A – Aluminum-bronze alloy block for up to 700 ^oC, vertically extended by steel tubes; B – Plate heat shields of stainless steel with holes for D and some also with holes for E, fixed with nuts (not all shown); C – Brass jacket containing quartz wool insulation and with internal water-cooling copper coil; D – Treaded stainless steel rods for fixing of B plates; E – Ampoule, see Fig. 2; F – Outer quartz windows for collection of scattered light and inspection; G – Small quartz windows for laser light illumination (projection); H – Inner windows (like F but smaller) for better temperature stabilisation and inspection; I – Separate heating coils for windows; J – Molten electrolyte (when heated) and platinum electrodes; K – Electrical feed through; L – Welding ball joining electrical wires; M – Rods D fixed to the bottom block that can be moved up and down by means of an elevation tooth bar; N – Heating coils, insulated; O – Silver cables with alumina pearls insulation; P – Bottom plate with holes to let cables O to come out and the elevation tooth bar to move; Q – Tooth wheel system for moving/fixing the tooth bar. Temperature sensors are not shown.

Vapor pressure. To obtain the H_2O partial pressures quantitative Raman spectra of the vapor above the salt were measured. The salt was contained in conveniently filled cells of Pyrex™ (~2mm wall thickness, ~16 mm internal diameter, see Fig. 2A). Wide round tubes were used; wide to avoid signals from the walls and round because they better stand up to high internal pressures.

After addition of the KH_2PO_4 to a cell it was connected via rubber tubing to a vacuum line (< 0.1 Torr), evacuated, repeatedly filled with a reference gas and sealed with a butane-oxygen torch. The reference gas needs to be inert and to have a strong Raman signal. Methane or hydrogen worked satisfactorily at a predetermined pressure of ~0.5 bar at 25 °C. We tried to use nitrogen as a reference gas, but this gas tended to give imprecise results, probably because the nitrogen signal from the laboratory air interfered. We could possibly have avoided this by using cells of square cross sections but the high internal pressure and **the risk of explosion** urged the use of another internal calibration gas. Fused quartz (silica) tube cells containing the salt, water and methane, were *not* used because of the limited stability of methane or hydrogen molecules; silica requires very high sealing temperatures (CH_4 or H_2 would decompose in the extreme heat). Enough salt was added to each cell so that concentration changes by loss of water to the gas phase could be neglected.

A.

B.

C.

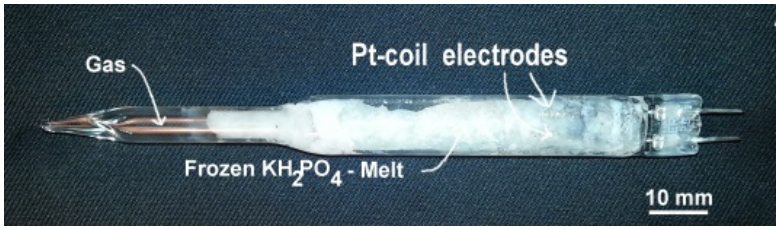

Fig. 2. Photographs of experimental ampoules for containing KH_2PO_4. A: Sealed vapor pressure cell of Pyrex™ (more than half filled) containing also methane, before heating. B: Empty electrolysis cell of fused quartz glass. C: Electrolysis cell, about half filled, evacuated and sealed, shown after being heated to melt the KH_2PO_4 and containing hydrogen and oxygen formed by electrolysis at 310 °C.

Water electrolysis. The new type of electrolysis cell of fused quartz glass (Fig. 2, B) was home-constructed in our glass-blowing workshop. The cells were made starting from standard silica halogen lamps adapted with platinum electrodes welded to the tungsten feedthrough wires and adding quartz glass tubes. At first the bulb of a new halogen lamp was cut open and the tungsten spiral was cut over – thereby creating the two electrode connections to which pre-wound platinum spirals were mechanically fixed and welded. Thereafter the whole cell was constructed by prolonging the quartz to form a tube and reducing the width for easy sealing. Such cells after connection to electric cables would allow electrolysis to be performed as well as simultaneous recording of Raman spectra of the melt and the gas phase at high temperatures inside the furnace by use of the elevation system (Fig. 1). Typical electrolysis ampoules are shown in Fig. 2, B and Fig. 2, C. Before use the empty cell in Fig. 2, B should be vacuum tested, filled with KH_2PO_4, evacuated, sealed, and mounted to the holder and connected with silver wire cables, electrically isolated by alumina beads, mounted inside the Raman furnace and heated. Electrolysis currents of about 5 mA were delivered through the cell by a Princeton Applied Research *VersaStat 3* potentiostat for several hours while *in situ* Raman spectra were recorded.

3. Results and discussion

Vapor pressure determination. The spectra of the vapor above the salt in a number of round tube cells of Pyrex™, more than half filled with the electrolyte chemicals, were recorded *versus* temperature. Methane or hydrogen had been added to the cells prior to sealing for use as internal pressure calibration standards. The recorded gas phase spectra were found to contain the expected well-known Q-branch rotational-vibration bands of methane (at ~2917 cm^{-1}, the ν_1 sym str band of CH_4) or hydrogen if added (at ~4156 cm^{-1}, the ν str rot-vib bands of H_2) in addition to the Q branch rot-vib band of the water molecules (at ~3655 cm^{-1} ν_1 sym str band of H_2O) originating from the salt, see Fig. 3. The presence of hydrogen could also be detected by means of the rotational lines at 354.4, 587.1, 814.4 and 1034.7 cm^{-1} [15]. All these bands are obvious in Fig. 3 showing an example spectrum of gases before and during water electrolysis, as discussed below.

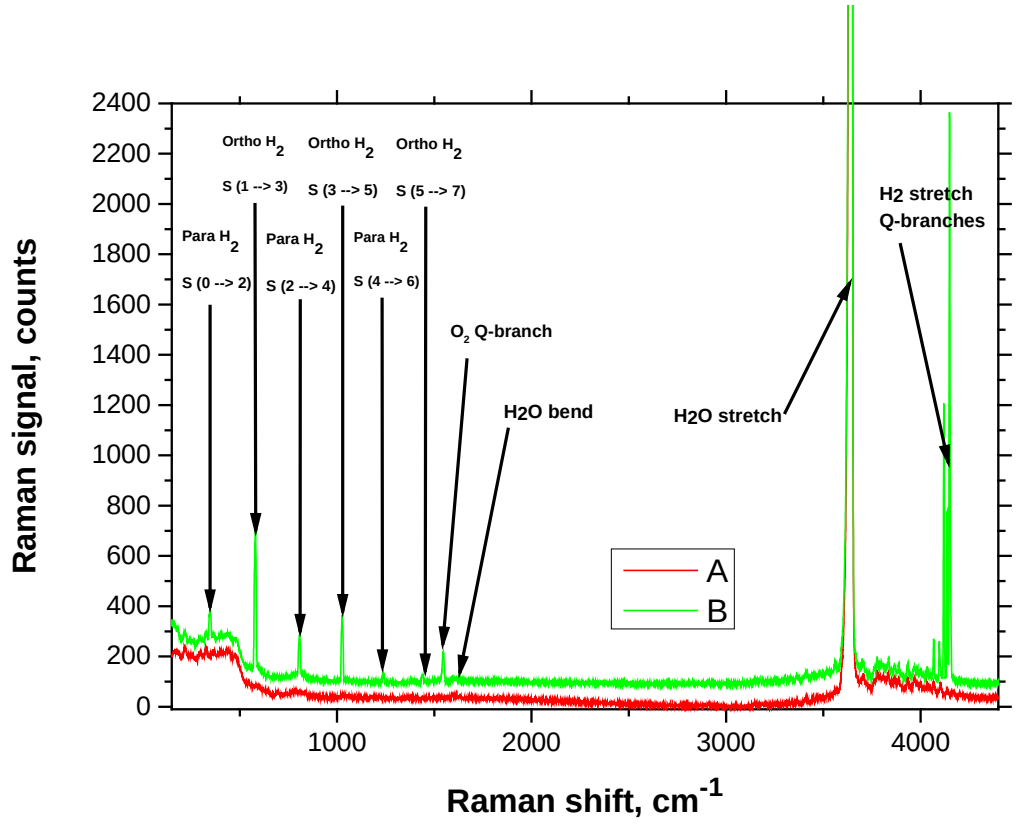

Fig. 3. Example of Raman spectra of the gas over molten KH_2PO_4 in a sealed ampoule before and during electrolysis at ~310 ^oC. A 532 nm laser was used to record the spectra. A: - Spectrum before start of electrolysis. B: Spectrum after about two hours of electrolysis. Electrolysis products, hydrogen (H_2) and oxygen (O_2), are visible by virtue of the new bands in B in addition to the bands from the vaporised water. The new bands comprise the well-known Raman gas Q branch lines at ~1555 cm^{-1} (O_2) and ~4150 cm^{-1} (H_2). The hot gas showed at least six hydrogen rotational S branch lines. No nitrogen line is observed, but a background from silica can be seen most pronounced below 600 cm^{-1}. Bands due to rotating water molecules are obvious in both A and B below 600 and near 4000 cm^{-1}.

The CH_4 or H_2 Raman bands can be used as internal intensity standard calibration signals, making it possible to quantify the water content by means of the intensity [16], as discussed in detail in [14] and [17-19]. In spite of the rather weak scattering strength, the Raman spectroscopy technique is a favorable method to determine the content of gases trapped in voids, because the signals are species-specific and the signal (intensity) should be linearly dependent on the species concentration. A necessary pre-requisite is the knowledge of scattering cross sections for characteristic bands of the molecules, here e.g. the ν_1 Q-branches of H_2O, CH_4 or H_2. A summary of the literature on intensity calibration is given in [14] and in works cited there. The conclusion of the discussion in [14] was that the ***molecular ratios*** of the water to reference scattering cross sections, $\sigma_{water}/\sigma_{reference}$, are needed. It was shown that $\sigma_{water}//\sigma_{methane}$ takes a value at around 0.4 (although different values have been given by different authors). For water to hydrogen the scattering ratio, $\sigma_{water}/\sigma_{hydrogen}$, takes a value at around 1.2. Considerable deviations among similar ratios given in the literature were seen. However, it was shown for the case of concentrated phosphoric acid [14] that the reference gases CH_4 and H_2 gave satisfying results by the Raman molecular scattering ration method.

The principle of how to determine the water pressure by the Raman bands depends on the scattering cross section *ratios*, e.g. $\sigma_{water}/\sigma_{methane}$, as explained in Fig. 4. We recorded e.g. the water and methane bands of cells with known contents of both substances and under equal experimental settings of the laser and the spectrometer. In this way we could determine the band areas, S_{water} and $S_{methane}$ for series of cells. We could then, for each cell and band, calculate the area per molecule. Since the experimental conditions are the same pairwise, the ratio between the areas *per gas molecule* is proportional to the *scattering cross section ratios*, e.g. $\sigma_{water}/\sigma_{methane}$. The cells contained only water and methane or only water and hydrogen in known amounts, made as explained in [14]. In this way values for $\sigma_{water}/\sigma_{methane}$ = ~0.40 ± 0.03 were found, when band contours were integrated over suitable ranges (~20 to ~100 cm^{-1}). The $\sigma_{water}/\sigma_{methane}$ was determined *vs.* temperature *T* and proved to be rather independent of temperature, up to ~350 °C, in fairly accordance with prior literature as described in detail in [14]. For $\sigma_{water}/\sigma_{hydrogen}$ values were found around ~1.20 ±0.03 depending somewhat on the range of integration and the temperature. The reason for the variability is supposed to be that at higher temperatures more hydrogen molecules are rotating with quantum number J = 2 or higher, making the reference not entirely constant.

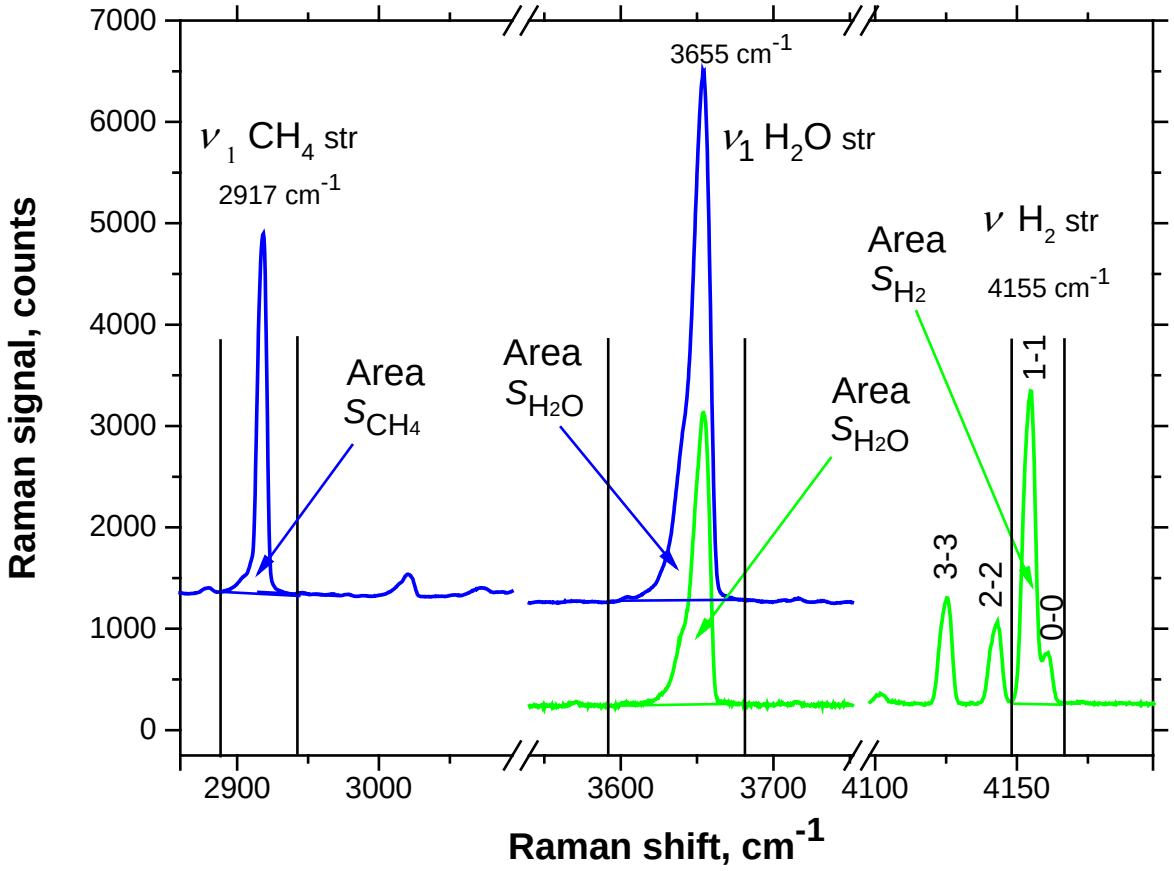

Fig. 4. Principle of Raman determination of water pressure inside sealed ampoules. By knowing e.g. the reference CH_4 pressure p_o at T_o, the water pressure p_{water} at *T* is given by $p_o \times (T/T_o) \times (S_{water}/S_{methane})/(\sigma_{water}/\sigma_{methane})$. *S* is a Raman signal area. The scattering cross section ratio, e.g. $\sigma_{water}/\sigma_{methane}$, between water and methane gas molecules exhibiting ν_1 Q-branch transitions was determined to be ~0.4, rather independent of temperature [14]. For hydrogen, an analogous expression is valid with $\sigma_{water}/\sigma_{hydrogen}$ being ~1.2. The used integration ranges were from ~2890 to ~2943 (CH_4), from ~3590 to ~3693 (H_2O) and from ~4149 to ~4169 cm^{-1} (H_2). A 532 nm laser was used to record the spectra.

Raman spectra from ampoules designed for estimating the water vapor pressure over the KH_2PO_4 salt versus temperature are given in Table 1. The pressures were evaluated as explained in Fig. 4 and the data are plotted graphically in Fig. 5. The establishment of the equilibrium took several hours; if measurements were taken immediately after a temperature change non-equilibrium resulted. According to these Raman results, the water vapor pressures over the molten KH_2PO_4 salt are considerable, around 8 bars at 300 °C.

Table 1. Calculated vapor pressures over KH_2PO_4 salt in sealed ampoules containing also 0.5 bar of the reference gas, either methane or hydrogen. The calculation of the pressure is based on an assumption that the reference is not reacting with nor absorbed/dissolved in the salt.

Temperature, °C	Observed water vapor pressure, bar		
	First CH_4 ampoule	Second CH_4 ampoule	H_2 ampoule
50		0.028	
53			0.230
70		0.095	
79			0.276
90		0.190	
105	0.42		0.442
110		0.286	
130		0.396	
131			0.910
150		1.331	
155	0.94		
162			1.311
170		1.811	
189			1.887
190		3.205	
205	3.20		
210		3.991	
215			2.128
230		4.013	
231			2.490
250		4.018	
252			2.270
255	4.24		
265		4.070	
273			2.506
280	6.08	4.816	
290		5.824	
294			5.441
300		7.412	8.037
305	10.92		
310		9.512	
315	12.53		
320		11.501	
325	14.66		

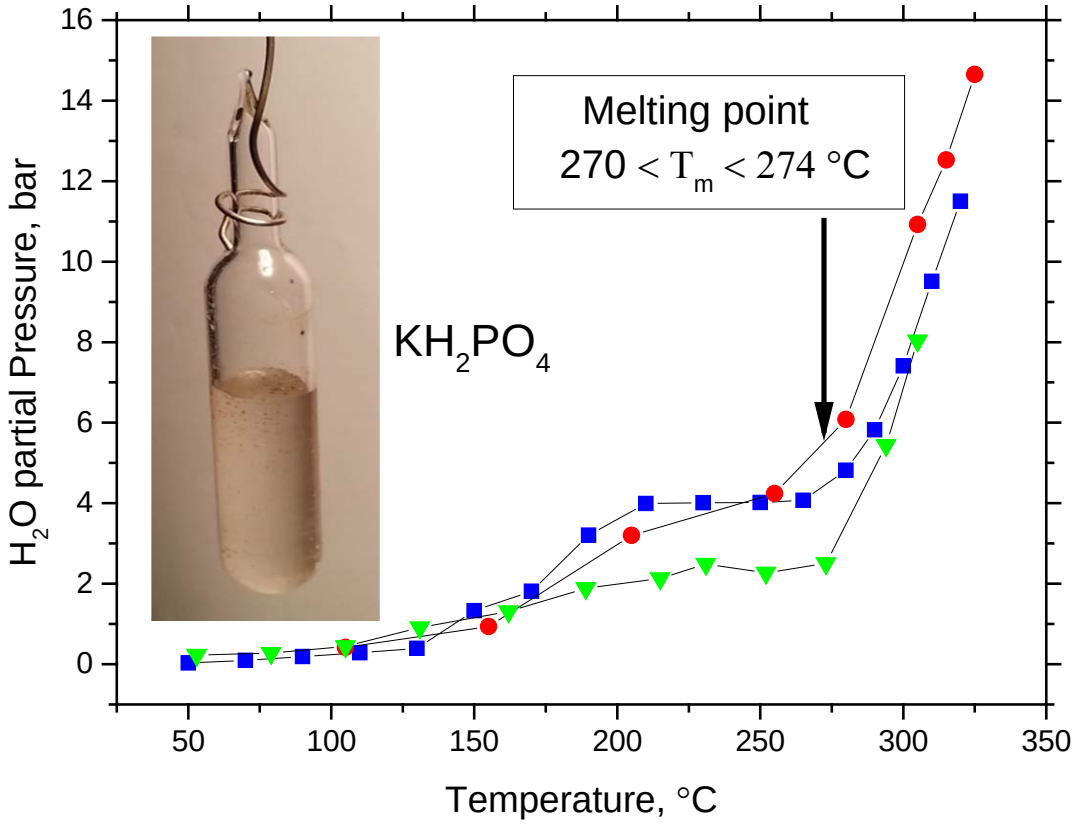

Fig. 5. Found Vapor pressure curves over KH_2PO_4 in sealed ampoules *vs.* temperatures. During heating the pressure reaches a halt at ~200 °C and the pressure stays rather constant up to the melting point at about 272 °C. Establishment of equilibrium was allowed for several hours or days during which periods the pressure slowly increased; if measurements were taken immediately after a temperature change too low values resulted. The inserted photograph shows a cell with a melt and a gas at ~310 °C, lifted out of the furnace for a moment. One should be aware of the considerable risk of an explosion during such an activity.

Raman spectra of the solid or liquid KDP versus temperature. The Raman spectra of KDP phases have been studied many times in previous literature in dependence of conditions such as temperature, pressure, chemical composition and preparation techniques. Limiting ourselves here to Raman spectra at room and higher temperatures there are still many studies available [20-35]. There is a consensus that the crystal structure at room temperature is tetragonal (space group $I\bar{4}2d$) and that the structure transforms to monoclinic (space group $P\bar{1}$, $P2_1/c$ or $P2_1/m$) at temperatures at about 180-200 °C. The transformation to this lower symmetric phase is well documented by many techniques and the decomposition of the KH_2PO_4 to KPO_3 + H_2O has been taken into account, see e.g. [21,24,25,28-31,33]. The room temperature Raman bands of KH_2PO_4 have been assigned carefully, based on orientated single crystal studies at room temperature [21,26-27,30-31] and calculations have been also done [36]. Spectra at higher temperatures in the monoclinic phase similar to our spectra have been obtained before [24,25,28,29,33,34], including a peak at 1175 cm^{-1}. The broad peaks at about 1830, 2390 and 2710 cm^{-1} have also been seen [20,33,34] and were related to the intermolecular hydrogen bond network. Signs of dehydration composition were seen at high temperatures and pressures [28,29], and it may be that there exists another solid phase before the melting.

We made Raman studies of the electrolyte as shown in Fig. 6. The elevation system described in Fig. 1 was used to facilitate this to make sure that the phase spectra corresponded to the particular temperature and pressure. When estimating the amount of water in the gas phase above the melt, using the ideal gas law, we calculated that more than 90% of the content of water remained in the melt. When the melt was quenched large crystals resulted, having spectra similar to the original spectrum (see top of Fig. 6) and after equilibration no water remained in the gas phase, that had essentially a spectrum with little water like before the heating. This means that the 25 °C spectrum is reversible after heating and cooling, as also noted by [21] after several days in open air.

When melting occurred the spectrum changed as shown in Fig. 6. To our knowledge this is the first recorded spectra of the melt under it decomposition pressure. The most characteristic change is the appearance of a new band at 710 cm^{-1}. This band assigned as due to protonated $[P_2O_7]^{4-}$ units (pyrophosphate), and sign of its formation has been seen before during heating decomposing KH_2PO_4 by loss of water forming ½ $K_2H_2P_2O_7$ + ½ H_2O, see e.g. [25,28,29,33]. P-O-P stretching in pyrophosphates is known to occur at ~750 cm^{-1} in many salts, see e.g. [37].

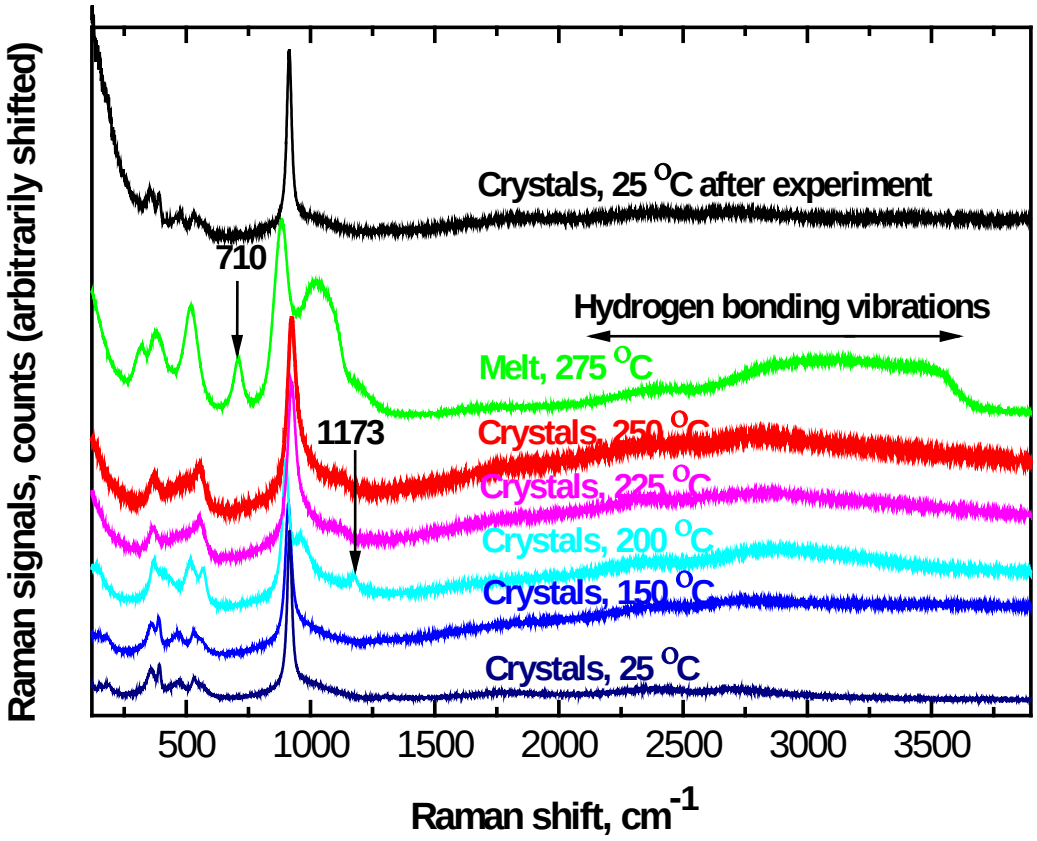

Fig. 6. Raman spectrum of the molten KH_2PO_4 in electrolysis ampoules obtained versus temperature up to ~275 °C. The solid spectra that were distinct at around 200 °C (band at 1173 cm^{-1}); at higher temperatures the solid spectra lost that peak and became simpler. The melts at ~275 to ~320 °C showed broad band envelopes at ~2000 to ~3500 cm^{-1} that are characteristic of OH hydrogen bond stretching. The spectral bands below ~1500 cm^{-1} are due to the phosphate and polyphosphate ions (710 cm^{-1}) in the electrolyte melt mixture containing water.

Water electrolysis. We made experiments to demonstrate that water electrolysis could indeed be done. The current was successfully passed from the power supply *via* the Pt electrodes through the molten KH_2PO_4. In this way it was demonstrated, by Raman spectroscopy, that molecules of hydrogen and oxygen could indeed be formed and released to the gas phase, at ~280 to ~325 °C (we did not dare to go to higher temperatures). A typical gas phase spectrum is shown in Fig. 3. All the obtained gas spectra were characteristic in containing the well-known Raman band rot-vib Q branches at ~4156 (H_2), ~1555 (O_2), and ~3655 cm^{-1} (H_2O) and the H_2 rotational bands in the range at 200-1500 cm^{-1} [15, 17]. Also, no other gases seemed to be formed. The amount of H_2 relative to O_2 seems to be like the expected 2 to 1 ratio; the O_2 signal being so small because of the known small Raman scattering cross section of O_2 relative to those of H_2. The situation is however complicated by the presence of hydrogen as para-H_2 and ortho-H_2, see e.g. [15,38]. The relative stability of the 2 H_2 + O_2 molecular mixture towards reformation of water at the temperature probably is due to the simultaneous presence of the water molecules that reduce the speed. If the back reaction:

$2\ H_2 + O_2 \rightarrow 2\ H_2O$

occurs, the only thing happening will be the formation of water, and the presence of the water vapor adds nothing new to the gas phase spectra. But, the demonstration of the simultaneous presence of H_2 and O_2 molecules in the gas phase remains a fact.

Affinity of water to the melt. The vapor pressure of the steam in the gas was high (on the order of ~ 8 bars), see Fig. 5. But the gas volume was small and the amount of water in the gas phase was also small even at the high pressure; we estimate from using the ideal gas law that the majority (~90 mol %) of the H_2O formally present in the cells remained in the melt. Apparently the affinity of water for stay in the melt is very high, much higher than for H_2O molecules to remain liquid in water. This is manifested in that the Raman spectra of the melt showing the broad band envelope from ~2000 to ~3500 cm^{-1} due to the OH hydrogen bond stretchings, as indicated in Fig. 6.

The spectral bands below ~1500 cm^{-1} are due to the phosphate and polyphosphate ions in the melt mixture. The characteristic spectrum of pyrophosphate [O_3P-O-PO_3] stretching at ~710 cm^{-1} is interesting, as is the absence of any bands due to ring formation. The analysis of these results will be described in detail elsewhere.

By quenching the melts, mm-sized crystals were quickly formed, consisting of KH_2PO_4 (proved by Raman spectra from closed cells). This indicates that much water must be available inside the melts; otherwise there would not have been enough time for the growth of coarse crystals.

The amount of steam in the gas was slow to reach equilibrium (many hours). Yet, at equilibrium the limiting pressure was much lower than the corresponding vapor pressure above liquid water. Thus the affinity of water for being in the melt is high, and the majority of the formally present water remained in the melt.

Conclusions

The behavior of the KH_2PO_4 salt/melt electrolyte (melting at 272 ºC) was investigated at temperatures up to ~325 °C and under its own water vapor pressure. Raman spectra were obtained from almost full sealed cells showing that the water vapor inside closed cells can reach more than 8 bars. We have in our recent publication [1] found that the liquid KH_2PO_4 has a high conductivity of ~0.30 S cm^{-1} at 300 °C. Here we have by Raman spectroscopy demonstrated that electrolysis is possible whereby water molecules split to form only hydrogen and oxygen. Water has a high affinity for staying in the melt being bound by hydrogen bonds. The presence of the water in the melt causes the Raman spectrum of the melt to show a broad band envelope at ~2000 to ~3500 cm^{-1} due to OH stretching. By quenching the melt, mm-sized crystals were quickly formed, proven by Raman spectra to consist of KH_2PO_4. The crystallization means that the water must already be present in the liquid phase at the high temperature, because otherwise there would not be time for the coarse grain crystallization: The water must be available inside the melts. We conclude that we have found KH_2PO_4 to be a new potentially high efficiency electrolyte for intermediate temperature pressurized water electrolysis with great perspectives for development of efficient water electrolysis.

Safety. Please note that the internal pressures in the ampoules at high temperatures give **high risks of explosions.**

Acknowledgements

This investigation has been supported by the Danish National Advanced Technology Foundation, grant.nr. 068-2011-1 and the Danish Council for Strategic Research (Medium Temperature Water Electrolysers (MEDLYS)), grant no. 10-093906. The quartz cells were made by glass blowing by Mr. Jan Patrick Scholer.

References

[1] Nikiforov AV, Berg RW, Petrushina IM, Bjerrum NJ. Specific electrical conductivity in molten potassium dihydrogen phosphate KH_2PO_4 – an electrolyte for water electrolysis at ~300 °C. Applied Energy, accepted for publication, 2016.

[2] Nikiforov AV, Petrushina IM, Jensen JO, Bjerrum NJ. Corrosion behavior of construction materials for intermediate temperature steam electrolysers. Advanced Materials Research. 2013;699:596-605. Presented at: 2013 International Conference on Materials Science and Chemical Engineering (MSCE 2013),
Singapore. http://dx.doi.org/10.4028/www.scientific.net/AMR.699.596.

[3] Kiehl SJ, Wallace GH. The dissociation pressures of monopotassium and monosodium orthophosphates and of dipotassium and disodium dihydrogen pyrophosphates. Phosphate IV. J. Am. Chem. Soc. 1927;49:375-86.

[4] Farag HI, Elmanharawy MS, Abdel-Kader A. Some Temperature Dependent Properties of Potassium Dihydrogen Phosphate. Acta Phys. Hung. 1986;60 (1-2):19-30. Springer-Verlag. http://dx.doi.org/10.1007/bf03157413.

[5] Subramony JA, Lovell S, Kahr B. Polymorphism of Potassium Dihydrogen Phosphate. Chemistry of Materials. 1998; 10 (8): 2053-57. http://dx.doi.org/10.1021/cm980293j.

[6] Fragua DM, Castillo J, Castillo R, Vargas RA. New Amorphous Phase $K_nH_2P_nO_{3n+1}$ (n>> 1) in KH_2PO_4. Rev. LatinAm. Metal. Mater. Suplemento de la Revista Latinoamericana de Metalurgia y Materiales 2009; S1(2): 491-97.

[7] O'Keeffe M, Perrino CT. Proton conductivity in pure and doped KH_2PO_4. J. Phys. Chem. Solids. 1967; 28(2): 211-18. http://dx.doi.org/10.1016/0022-3697(67)90110-2.

[8] Perry DL. Handbook of Inorganic Compounds, 553 pages, Publisher: Taylor & Francis. 2011. ISBN: 1439814619, 9781439814611.

[9] Lewis RJ, Ed. Hawley's Condensed Chemical Dictionary, 12th ed. New York: Van Nostrand Reinhold Co. 1993.

[10] Merz AR. Note on Monopotassium Phosphate. J. Am. Chem. Soc. 1927; 49(6), 1511-12.

[11] Liu C, Berg RW. Determining the Spectral Resolution of a Charge–Coupled Device (CCD) Raman Instrument. Appl. Spectrosc., 2012; 66(9): 1034–43.

[12] Berg RW, Nørbygaard T. Wavenumber Calibration of CCD Detector Raman spectrometers controlled by a Sinus Arm Drive. Appl. Spectrosc. Rev. 2006; 41: 165–183.

[13] Berg RW, Maijó Ferré I, Schäffer SJC. Raman Spectroscopy Evidence of 1:1:1 Complex Formation during Dissolution of WO_3 in a Melt of $K_2S_2O_7$:K_2SO_4. Vibrat. Spectrosc. (Elsevier) 2006; 42: 346–52.

[14] Rodier M, Qingfeng L, Berg RW, Bjerrum NJ. Determination of Water Vapor Pressure over Corrosive Chemicals using Raman Spectroscopy: Exemplified by Application with a 85.5 % Phosphoric Acid. Appl. Spectrosc. 2016; xx: 1–9. Publ. on the internet, June 8, 2016. DOI: 10.1177/0003702816652362.

[15] Stoicheff BP. High Resolution Raman Spectroscopy of Gases IX. Spectra of H_2, HD, and D_2, Canad. J. Phys. 1957; 35: 730-41.

[16] Bribes JL, Gaufrès R, Monan M, Lapp M, Penney CM. Raman band contours for water vapor as a function of temperature. Appl. Phys. Lett. 1976; 28: 336–37.

[17] Schrötter HW, Klöckner HW. Raman scattering cross sections in gas and liquids. Topics in Current Physics, vol. 11, Raman Spectroscopy of Gases and Liquids, Editor A. Weber, Springer Verlag, New York. 1979: 123-66.

[18] Schrötter HW. Raman spectra of gasses. In B. Schrader: Infrared and Raman Spectroscopy. Methods and Applications, Wiley VCH, Weinheim, 1995: 277-96.

[19] Schrötter HW. Raman spectra of gasses. Chapter 8 in I.R. Lewis & H.G.M. Edwards: Handbook of Raman Spectroscopy. From the Research Laboratory to the Process Line. Practical Spectroscopy, series volume 28, Marcel Decker. 2001: 307-48.

[20] She CY, Pan CL. Raman scattering of high-temperature phase transition in KH_2PO_4. Solid State Commun. 1975; 17: 529-531.

[21] Serra KC, Melo FEA, Mendes Filho J, Germano FA, Moreira JE. Raman study of the tetragonal→ monoclinic phase transition in KDP. Solid State Commun. 1988; 66(6): 575-579.

[22] Dalterio RA, Owens FJ. A Raman scattering study of high-temperature phase transitions in potassium and rubidium dihydrogen phosphate. J. Phys. C.: Solid State Phys. 1988; 21: 6177-6185.

[23] Lee K-S. Hidden Nature of the High-Temperature Phase Transitions in Crystals of KH_2PO_4-Type: Is it a Physical Change? J. Phys. Chem. Solids 1996; 57(3): 333-342.

[24] Choi B-K. High-Temperature Phase Transitions of KH_2PO_4 Crystals. J. Korean Phys. Soc. 1998; 32(2): S515-S517.

[25] Subramony JA, Marquardt BJ, Macklin JW, Kahr B. Reevaluation of Raman spectra for KH_2PO_4 high-temperature phases. Chem. Mater. 1999; 11(5): 1312-1316.

[26] Lu G, Li C, Wang W, Wang Z, Guan J, Xia H, Lattice vibration modes and thermal conductivity of potassium dihydrogen phosphate crystal studying by Raman spectroscopy. Mater. Sci. Eng. B 2005; 116: 47-53.

[27] Liu WL, Xia HR, Wang XQ, Han H, Lu GW. Raman scattering from deuterated potassium dihydrogen phosphate crystals. Mater. Chem. Phys. 2005; 90: 134–138.

[28] Carr CW, Feit MD, Johnson MA, Rubenchik AM. Complex morphology of laser-induced bulk damage in $K_2H_{(2-x)}D_xPO_4$ crystals. Appl. Phys. Lett. 2006; 89: 131901-1 to 131901-3.

[29] Norman TJ, Zaug JM, Carr CW. High pressure decomposition of DKDP. Chem. Mater. 2006; 18: 3074-3077.

[30] Liu WL, Xia HR, Wang XQ, Ling ZC, J. Xu, Wei YL, Liu YK, Han H. Spectroscopic manifestation for the isotopic substitution in potassium dihydrogen phosphate, J. Alloys and Compounds 2007; 430: 226–231.

[31] Kawahata Y, Tominaga Y. Dynamical mechanism of ferroelectric phase transition in KDP/DKDP mixed crystals and distortion of PO_4 tetrahedron. Solid State Commun. 2008;145: 218-222.

[32] Botez CE, Carbajal D, Adiraju VAK, Tackett RJ, Chianelli RR. Intermediate-temperature polymorphic phase transition in KH_2PO_4: A synchrotron X-ray diffraction study. J. Phys. Chem. Solids 2010; 71:1576–1580.

[33] Jurado JF, Vargas-Hernández C, Vargas RA. Raman and structural studies on the high-temperature regime of the KH_2PO_4-$NH_4H_2PO_4$ system. Mexican J. of Physics (Rev. Mex. Fis.) 2012; 58: 411-416.

[34] Ettoumi H, Gao Y, Toumi M, Mhiri T. Thermal analysis, Raman spectroscopy and complex impedance analysis of Cu^{2+} doped KDP. Ionics 2013; 19: 1067-1075.

[35] Guo D, Jiang X, Huang J, Wang F, Liu H, Zu X. Effect of UV Laser Conditioning on the Structure of KDP Crystal. Adv. Condensed Matter Phys. 2014; Article ID 451048, 7 pages. http://dx.doi.org/10.1155/2014/451048.

[36] Rudolph WW, Irmer G. Raman and infrared spectroscopic investigations on aqueous alkali metal phosphate solutions and density functional theory calculations of phosphate-water clusters. Appl. Spectrosc. 2007; 61(12): 1312-1327.

[37] Kowada Y, Adachi H, Tatsumisago M, Minami T. Raman spectra of rapidly quenched lithium pyrophosphate glass at various temperatures. Phys. Chem. Glasses 1993; 34(1): 10-11.

[38] Petitpas G, Aceves SM, Matthews MJ, Smith JR. Para-H_2 to ortho-H_2 conversion in a full-scale automotive cryogenic pressurized hydrogen storage up to 345 bar. Internl. J. Hydrogen Energy 2014; 39: 6533-47.